

Tuning Dimensional Order in Self-Assembled Magnetic Nanostructures: Theory, Simulations, and Experiments

Yulan Chen,^{*a}, Hanyu Alice Zhang,^b and Amal El-Ghazaly^{*c}

^a*Department of Materials Science and Engineering, Cornell University, Ithaca, New York 14853, USA. E-mail: yc2555@cornell.edu*

^b*School of Applied and Engineering Physics, Cornell University, Ithaca, New York 14853, USA.*

^c*School of Electrical and Computer Engineering, Cornell University, Ithaca, New York 14853, USA. E-mail: ase63@cornell.edu*

1 Experimental Methods

1.1 Material selection

FeCl₂ (99.5%, BeanTown Chemical), Co(Ac)₂·4H₂O (97%, Acros Organics), NaOH (Sigma-Aldrich), and ethylene glycol (Thermo Scientific) were analytical grade and used as received without further purification. Ethanol (Fisher Scientific) was used for the washing process after synthesis.

1.2 Synthesis of FeCo nanostructures with different dimensions

All syntheses were carried out under nitrogen gas flow to ensure minimal oxidation of the FeCo. Precursor quantities of 0.01 M FeCl₂ and 0.01 M Co(Ac)₂·4H₂O were dissolved in 100 ml ethylene glycol and magnetically stirred at 300 rpm for 30 min. Then, various amounts of NaOH (1.0, 2.0, 2.4, 3.2, and 4.0 M) were added to the metal salt solution. The resultant mixture was heated to and maintained

at 130°C for 1 h. The color of the mixture changed from orange to black during the process. After it was cooled down naturally to room temperature, the product was separated by a permanent magnet and washed with ethanol more than 3 times to remove the impurities and byproducts. The final product was stored in ethanol for further characterization. Based on the NaOH concentration, the samples were denoted as S0, S1, S2, S3, and S4, respectively.

1.3 Characterization

For the characterization of magnetically aligned samples, samples ($\sim 5 \text{ mg mL}^{-1}$) were deposited on $5 \times 5 \text{ mm}^2$ silicon wafer pieces situated on top of a bar magnet such that the solution dries while the nanostructures are organized in the presence of an external in-plane magnetic field. A field emission scanning electron microscope (FE-SEM) Zeiss Gemini 500 was used to observe morphology. The elemental composition was examined by energy dispersive X-ray (EDX) spectrometry. Transmission electron microscopy (TEM) was carried out with a FEI Tecnai 12 BioTwin instrument. A Bruker D8 Advance ECO powder X-ray diffractometer (XRD) was used for crystal structure analysis. The scanning range was from 20° to 90° using Cu $K\alpha$ radiation. The hysteresis loops of the samples at room temperature were measured using a vibrating sample magnetometer (VSM, Lakeshore 8600). The magnetic force microscopy (MFM) observations were conducted by a Veeco Dimension Icon atomic force microscope.

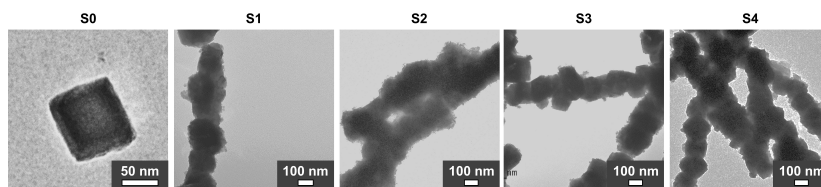


Fig. S1 TEM images showing samples synthesized under various $[\text{OH}]/[\text{M}]$ ratios and drop-cast without the application of a magnetic field.

2 Structural Characterization Results

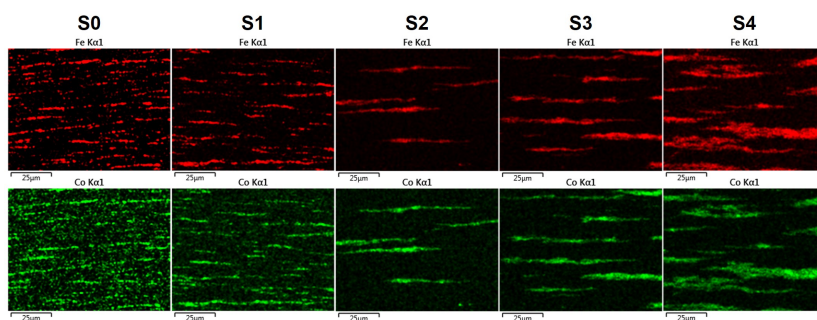


Fig. S2 EDX maps for samples synthesized under different $[\text{OH}]/[\text{M}]$ ratios.

3 Simulation Results

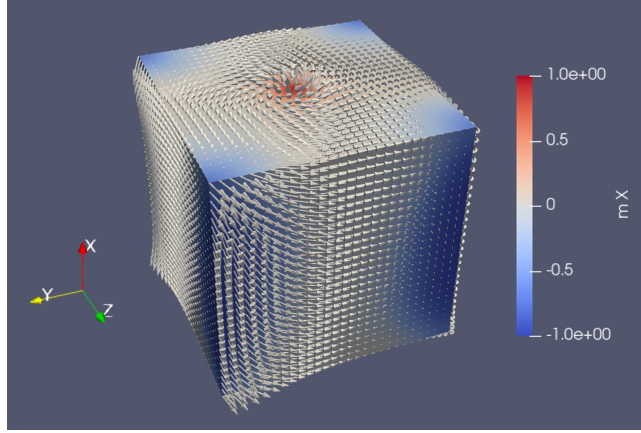


Fig. S3 Simulated magnetic spin state of a cubic nanoparticle with an edge length of $L = 140$ nm.

To determine the net magnetization direction, we first simulated the equilibrium configuration of an individual FeCo cube measuring 140 nm, the same size as the cubes forming the chain in S1. We then calculated the net magnetization (1938 emu/cc) as the vector sum of the spins at equilibrium and determined the cosine of the angle between the net magnetization and $[100]$, which turned out to be 0.05° . The details of the simulation methods were previously reported elsewhere¹.

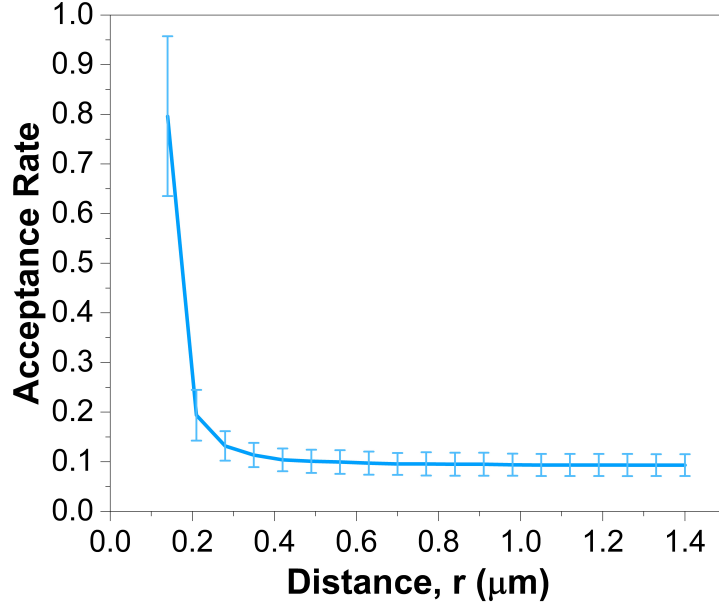


Fig. S4 The acceptance rate as a function of distance, r , between a new particle and the end of the existing chain. Results shown are for a particle of size $L = 140$ nm and thermal energy $k_b T = 1 \times 10^{-15} J$. For each separation distance, the data points and error bars indicate the average and standard deviation, respectively, of the different acceptance rate values observed throughout the chain formation. In other words the spread shows the range of acceptance rates resulting from an existing chain of just 1 particle up to the maximum of 19 particles, with the new particle being added at the given distance r from that chain.

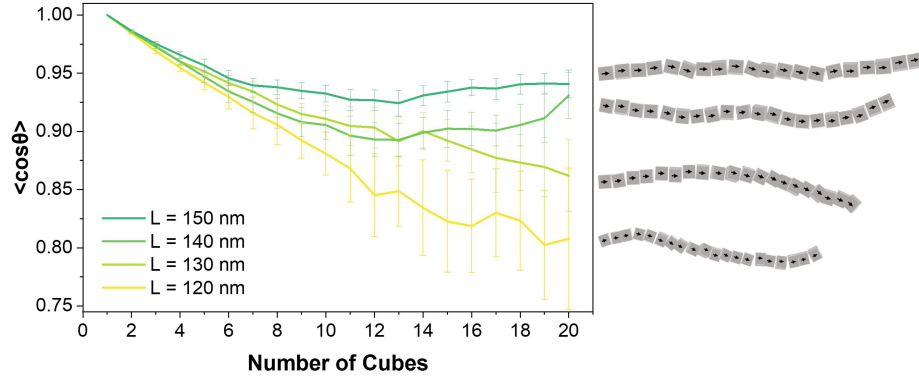


Fig. S5 Simulated zigzag angle and corresponding chain geometry as a function of number of MNPs with particle size $L = 120, 130, 140$, and 150 nm, and $k_b T = 1 \times 10^{-15} J$. The right panel presents 3D rendering of chains corresponding to each particle size in the graph.

4 Magnetic Characterization

Table S1 Comparison of magnetic properties for FeCo structures synthesized in this study and in our previous work².

Sample	M_S (emu g ⁻¹)	M_R (emu g ⁻¹)
S0	218	24
S1	216	45
S2	216	58
S3	215	65
S4	210	69
Prior Work ²	220	20

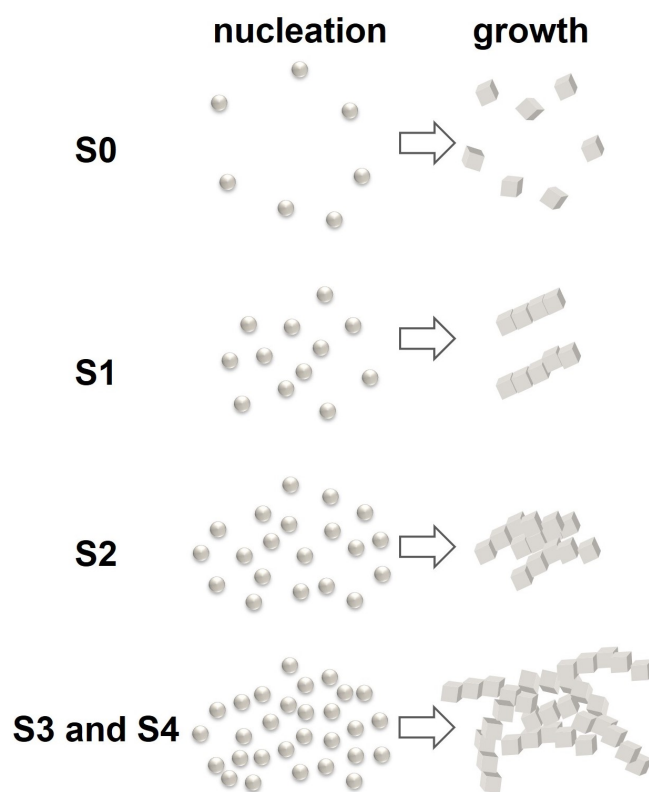


Fig. S6 Schematic illustration of the growth mechanism of the FeCo nanostructures synthesized under different $[\text{OH}]/[\text{M}]$ ratios.

References

- [1] Y. Chen and A. El-Ghazaly, *Small*, 2023, **19**, 2205079.
- [2] Y. Chen, K. Srinivasan, M. Choates, L. Cestarollo and A. El-Ghazaly, *Advanced Functional Materials*, 2024, **34**, 2305502.